MAGNETIC ROTATION IN ^{60}Ni: A SEMICLASSICAL DESCRIPTION

S. Ganguly†

Department of Physics, Bethune College, Kolkata, India

C. Majumder, S.S. Tiwary, H.P. Sharma

Department of Physics, Institute of Science, Banaras Hindu University
Varanasi, India

S. Chakraborty

Nuclear Physics Group, Inter-University Accelerator Centre, New Delhi, India

(Received September 15, 2019; accepted December 4, 2019)

Semi-classical particle rotor model calculation has been carried out for the magnetic dipole bands in ^{60}Ni to understand the possible existence of the shears mechanism in this nucleus. The reduced transition probability of the magnetic dipole transitions belonging to the candidate magnetic rotational bands has been calculated. Results of the present work have been discussed in the light of the earlier theoretical works on this nucleus.

DOI:10.5506/APhysPolB.51.473

1. Introduction

Observation of rotational-like sequence of magnetic dipole (M1) γ transitions in nearly spherical nuclei interpreted under the framework of shears mechanism has attracted a significant interest for last few decades [1–3]. This type of sequence exhibits a strong B(M1) strength and a small B(E2), resulting in a large B(M1)/B(E2) value. Such a kind of band structure has originated due to the symmetry breaking by the current distributions of a few high-spin particles and holes outside a weakly deformed core and also by the magnetic moments associated with these currents. As the magnetic moment breaks the symmetry and rotates around the angular momentum

† Corresponding author: sgpresi78@gmail.com

vector, this mode of nuclear excitation is known as a "magnetic rotation" (MR) [4, 5]. The excitation energy of a magnetic rotational band increases by the step-by-step alignment of particle or hole spins in the direction of the total angular momentum, as shown in Fig. 1. The other fingerprint of this phenomena is the low dynamic moment of inertia ($\lessapprox 35\ \hbar^2\ \mathrm{MeV}^{-1}$), which remains constant with spin. Magnetic rotational bands were reported in more than 200 nuclei throughout the nuclear chart [6]. Most of the cases were reported in $A \approx 110$, 200 regions [6]. However, abundance of such bands in $A \approx 60$ was found smaller. A semiclassical description of the shears mechanism [3] was given by Macchiavelli and Clark [7, 8] and it was further extended for the twin shears mechanism [9] by Sugawara *et al.* [10]. This model is successfully used to study the shears and the twin shears bands in several nuclei [11–28].

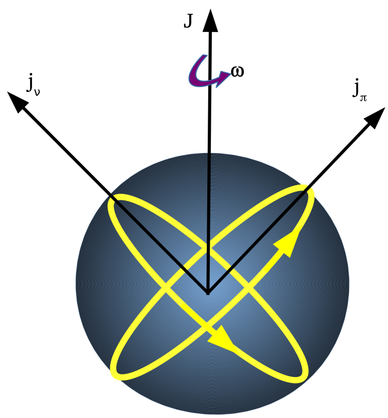

Fig. 1. Generation of the angular momentum in an atomic nucleus through shears mechanism [2].

Four sequences of M1 transitions were reported in ^{60}Ni (marked as M-1, M-2, M-3, and M-4 in Ref. [29]) and interpreted as the MR bands on the basis of Cranked Nilsson–Strutinsky (CNS) calculations. This makes ^{60}Ni one of the lightest systems in which MR bands were observed. Later, the self-consistent tilted axis cranking relativistic mean-field (TAC-RMF) theory based on a point-coupling interaction was carried out to study the candidate shears bands in ^{60}Ni [30]. From that calculation, it was concluded that the competition between the configurations and the transitions from the magnetic to the electric rotations has to be considered in order to reproduce the energy spectra as well as the band crossing phenomena. In the present work, an attempt has been made to study these bands in the framework of semiclassical particle rotor model (SCM).

2. Formalism

A semiclassical description of the shears mechanism, originally proposed by Frauendorf using the tilted-axis-cranking model [3], was given by Macchiavelli *et al.* [7], where the energy states of a shears band were generated from the interaction of particles and holes. This interaction is proportional to $P_2(\theta)$, where θ is the shears angle between j_π and j_ν, defined as

$$\cos\ \theta = \frac{\vec{j_\pi} \cdot \vec{j_\nu}}{\mid \vec{j_\pi} \mid \cdot \mid \vec{j_\nu} \mid} = \frac{I_{\rm sh}(I_{\rm sh}+1) - j_\pi(j_\pi+1) - j_\nu(j_\nu+1)}{2\sqrt{(j_\pi(j_\pi+1)j_\nu(j_\nu+1))}}\,, \qquad (1)$$

where $\vec{I}_{\rm sh}$ is the shears contribution of the total angular momentum $\vec{I}$ ($\vec{I}_{\rm sh} = \vec{j_\pi} + \vec{j_\nu}$). The total spin of the band $\vec{I} = \vec{I}_{\rm sh} + \vec{R}_{\rm core}$. The $\vec{R}_{\rm core}$ is the core contribution of the shears band.

The small effect due to the contribution of core in angular momentum towards total angular momentum can be determined by

$$R_{\rm core} = \frac{\Delta R}{\Delta I}(I - I_{\rm bh}) = \frac{I_{\rm max} - j_\pi - j_\nu}{I_{\rm max} - I_{\rm bh}}(I - I_{\rm bh})\,, \qquad (2)$$

where $I_{\rm max}$ is the maximum observed spin, $I_{\rm bh}$ is the band head of the shears band and I is the angular momentum of a particular state.

The interaction potential between the interacting particles and holes can be calculated from the excitation energy relative to the band-head energy and the angles between the holes and particles

$$\Delta E(I) = V_0 \frac{3\cos^2\theta - 1}{2}\,, \qquad (3)$$

where $\Delta E(I)$ is the difference between the energy of a particular level and the energy of the band head *i.e.*, $E(I) - E_{\rm bh}$. By calculating the shears angle, the interaction potential can be deduced.

The magnitude of $B(\mathrm{M1})$ is proportional to the square of the perpendicular component magnetic moment vector ($\mu_\perp$) [7]. The $B(\mathrm{M1})$ value can be calculated for each energy state and is given by

$$B(\mathrm{M1}, I \to I-1) = \frac{3}{8\pi} g_{\rm eff}^2 j_\pi^2 \sin^2\theta_\pi \left[\mu_N^2\right]\,, \qquad (4)$$

where j_π is the proton angular momentum, θ_π is the proton angle between j_π and total angular momentum I. The magnitude of θ_π is given by

$$\theta_\pi = \tan^{-1} \frac{j_\nu \sin\theta}{j_\pi + j_\nu\cos\theta}\,, \qquad (5)$$

where $g_{\rm eff}$ is the effective gyromagnetic factor given by $g_\pi - g_\nu$. The values of g_π and g_ν depend on the orbital involved at the configuration of the band.

3. Results and discussions

Four sequences of magnetic dipole transitions, marked as M-1, M-2, M-3 and M-4 in Ref. [29], have been studied in the framework of semiclassical particle rotor model. The Fermi surface of the proton–hole is near $\pi f_{7/2}$ orbital in this nucleus and that for the neutron particles is near the $\nu g_{9/2}$ and fp orbitals. The M-1 bands in ^{60}Ni were supposed to originate due to these orbitals. Two out of these four bands, namely M-1 and M-4, have negative parity and the other two, M-2 and M-3, have positive parity. The pair of positive (negative) parity bands has nearly the same excitation energy and angular momentum at the band head, as shown in Fig. 2. Consequently, bands M-1 and M-4 were suggested to have the

$$\pi\left(f_{7/2}^{-1}\right)(fp)^1 \otimes \nu\left(g_{9/2}\right)(fp)^3 \quad \text{(Config. 1)}$$

configuration and bands M-2 and M-3 were suggested to have either

$$\pi\left(f_{7/2}^{-1}\right)(g_{9/2}) \otimes \nu(g_{9/2})(fp)^3 \quad \text{(Config. 2)}$$

or

$$\pi\left(f_{7/2}^{-1}\right)(fp)^1 \otimes \nu(g_{9/2})^2(fp)^2 \quad \text{(Config. 3)}$$

configuration [29]. Here, the fp orbital describes the $1f_{5/2}$, $2p_{3/2}$ or $2p_{1/2}$ orbitals. Earlier, these four MR bands were studied in the framework of self-consistent tilted axis cranking relativistic mean-field (TAC-RMF) theory based on a point-coupling interaction [30]. In this work, the shears mechanism of the four bands has been studied by considering the same configuration.

For Config. 1, the magnitude of j_π and j_ν are taken as $6\,\hbar$ and $9\,\hbar$. The maximum spin that can be produced by the coupling of these two angular momenta is

$$(7/2+5/2+9/2+9/2)\,\hbar = 15\,\hbar\,.$$

These values of proton and neutron angular momentum are used in this work to calculate the shears angle and the proton angle of each states. The B(M1) values of each state have been deduced from the calculated proton angle.

The dynamic moment of inertia $[\Im^{(2)} = \frac{\mathrm{d}I}{\mathrm{d}\omega} = \frac{2}{\Delta E_\gamma}]$ of the band M-1, as shown in the inset of Fig. 3, is found quite low and also nearly constant as a function of angular momentum. This feature indicates a quite low deformation of the band and also serves as one of the fingerprint of the magnetic rotational nature of this band. Experimentally deduced $B(\mathrm{M1})/B(\mathrm{E2})$ values of the states belonging to this band are found quite high as shown in

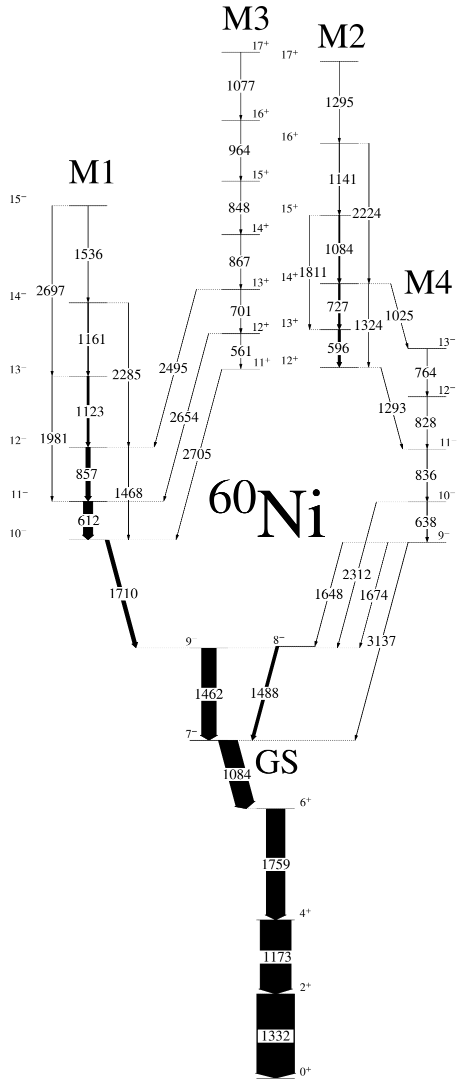

Fig. 2. Partial level scheme of ^{60}Ni showing the MR bands reported in Ref. [29].

Fig. 3 [29]. These two observations suggest that the shears mechanism is mainly responsible for the generation of angular momentum in this band. Therefore, the theoretical semiclassical particle rotor model calculation has been carried out to understand the structure of this band. In this context, it may be noted that although the band M-4 having same configuration of band M-1 can also be explained in the framework of the shears mechanism, the dynamic moment of inertia of band M-4 is not very supportive to the rotational character of this band.

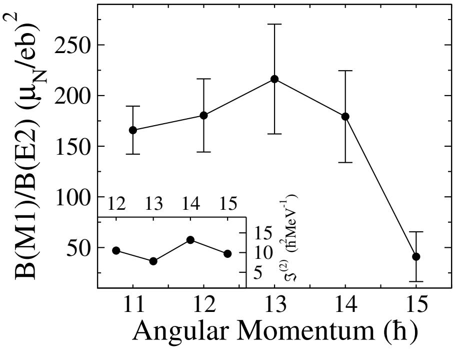

Fig. 3. Plot of the experimental $B(\mathrm{M1})/B(\mathrm{E2})$ and (inset) the dynamic moment of inertia $[\Im^{(2)}]$ as a function of angular momentum for the band M-1 in ^{60}Ni. Experimental data was taken from Ref. [29].

Config. 2 and Config. 3 mostly give rise to a similar shears angle and $B(\mathrm{M1})$ values of the states. The magnitude of j_π (j_ν) is taken as $8\,\hbar$ ($6\,\hbar$) for Config. 2 and $9\,\hbar$ ($10\,\hbar$) for Config. 3. The only difference between the two alternative configurations is the core angular momentum (I_{core}), which is $1\,\hbar$ for the Config. 2 and $0\,\hbar$ for Config. 3.

In the present work, the shears angle of each state has been calculated using Eq. (1), which (also, the proton angle) is found to decrease gradually with increasing spin for all three configurations. At the band head, the shears angle is maximum and it decreases with the increasing angular frequency. Generation of angular momentum due to the shears mechanism takes place in between $11\,\hbar$ and $15\,\hbar$ within the Config. 1. Similarly, for Config. 2 (Config. 3), it takes place from $12\,\hbar$ to $17\,\hbar$ ($16\,\hbar$). This indicates a pure shears contribution of the band from $11\,\hbar$ to $15\,\hbar$ for Config. 1, where the core contribution is negligible. The reduced transition probability of the magnetic dipole transitions $[B(\mathrm{M1})]$ show a decreasing trend with increasing angular momentum of the bands, as shown in Fig. 4. All the features, the low and constant dynamic moment of inertia, the decreasing shears angles with increasing spin, and the decreasing trend of $B(\mathrm{M1})$ with increasing angular momentum indicate the magnetic rotational nature of the (M-1–M-4) dipole bands in ^{60}Ni. The interaction potential $[V(I(\theta))]$ has been calculated using Eq. (3) for M-1 and M-2 bands, as shown in Fig. 5. The magnitude of $V(I(\theta))$ is found ≈ 800 keV for these bands.

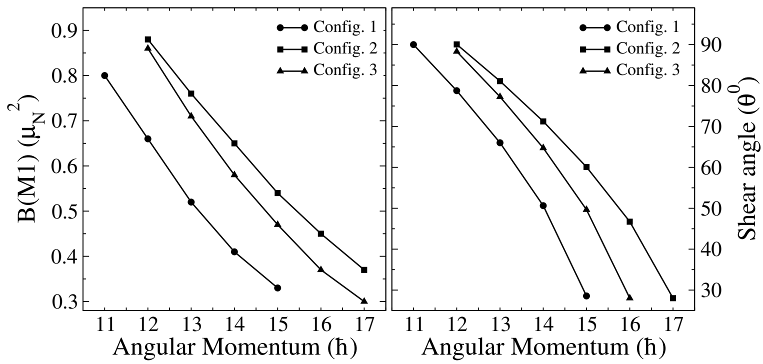

Fig. 4. Plots of (left) B(M1) and (right) shears angle (θ^0) as functions of angular momentum for the states of MR band of present interest in ^{60}Ni estimated from the semiclassical particle rotor model calculation.

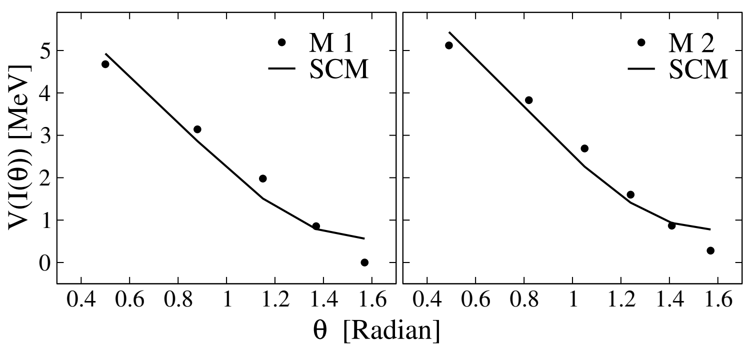

Fig. 5. Plot of the interaction potential as a function of shears angle for the M-1 and M-2 bands.

4. Summary

Theoretical semiclassical particle rotor model calculation has been carried out for four previously reported magnetic dipole bands in ^{60}Ni. The decreasing trend of the reduced transition probability of the magnetic dipole transitions [B(M1)] with increasing spin, derived from the present calculation suggest that the shears mechanism is responsible for the generation of angular momentum for these four bands. The trend and the magnitude of B(M1) is also found in agreement with the previously reported results of TAC-RMF calculation.

The first author acknowledges Prof. Dr. Mamata Ray Chaudhuri, Principal, Bethune College, Kolkata, India for her constant encouragement and support.

REFERENCES

[1] G. Baldsiefen *et al.*, *"Shears bands" in ^{199}Pb and ^{200}Pb*, Nucl. Phys. A **574**, 521 (1994).

[2] S. Frauendorf, *Spontaneous symmetry breaking in rotating nuclei*, Rev. Mod. Phys. **73**, 463 (2001).

[3] S. Frauendorf, *Tilted cranking*, Nucl. Phys. A **557**, 259 (1993).

[4] A.A. Raduta, *Specific features and symmetries for magnetic and chiral bands in nuclei*, Prog. Part. Nucl. Phys. **90**, 241 (2016).

[5] R.M. Clark, A.O. Macchiavelli, *The shears mechanism in nuclei*, Annu. Rev. Nucl. Part. Sci. **50**, 1 (2000).

[6] Amita *et al.*, *Table of magnetic dipole rotational bands*, At. Data Nucl. Data Tables **74**, 283 (2000).

[7] A.O. Macchiavelli *et al.*, *Semiclassical description of the shears mechanism and the role of effective interactions*, Phys. Rev. C **57**, 1073(R) (1998).

[8] A.O. Macchiavelli *et al.*, *Rotational-like properties of the shears bands*, Phys. Rev. C **58**, 3746 (1998).

[9] S. Frauendorf, in: Proc. of Workshop on Gammasphere Physics, World Scientific, Singapore 1995, p. 272.

[10] M. Sugawara *et al.*, *Possible magnetic and antimagnetic rotations in ^{144}Dy*, Phys. Rev. C **79**, 064321 (2009).

[11] P. Banerjee *et al.*, *Experimental study of $\Delta I = 1$ bands in ^{111}In*, Phys. Rev. C **83**, 024316 (2011).

[12] P. Banerjee *et al.*, *Spectroscopy of weakly deformed bands in ^{87}Zr: First observation of the shears mechanism in a Zr isotope*, Phys. Rev. C **98**, 034320 (2018).

[13] S. Roy *et al.*, *Band crossing in a shears band of ^{108}Cd*, Phys. Rev. C **81**, 054311 (2010).

[14] D. Choudhury *et al.*, *Role of neutrons in the coexistence of magnetic and antimagnetic rotation bands in ^{107}Cd*, Phys. Rev. C **91**, 014318 (2015).

[15] K.R. Devi *et al.*, *Geometry of magnetic rotational (MR) band-crossing phenomenon in MR bands*, Pramana **91**, 8 (2018).

[16] S. Ganguly *et al.*, *Shears mechanism in ^{113}in using semiclassical method*, *Int. J. Pure Appl. Phys.* **7**, 203 (2011).

[17] D. Choudhury *et al.*, *Evidence of antimagnetic rotation in odd-A ^{105}Cd*, Phys. Rev. C **82**, 061308(R) (2010).

[18] D. Choudhury *et al.*, *Multiple antimagnetic rotation bands in odd-A ^{107}Cd*, Phys. Rev. C **87**, 034304 (2013).

[19] P. Datta *et al.*, *Observation of antimagnetic rotation in ^{108}Cd*, Phys. Rev. C **71**, 041305(R) (2005).

[20] C. Majumder *et al.*, *Study of antimagnetic rotation in ^{109,111}Cd*, Int. J. Mod. Phys. E **27**, 1850034 (2018).

[21] S. Roy *et al.*, *Systematics of antimagnetic rotation in even–even Cd isotopes*, *Phys. Lett. B* **694**, 322 (2011).

[22] S. Roy, S. Chattopadhyay, *Possibility of antimagnetic rotation in odd-A Cd isotopes*, *Phys. Rev. C* **83**, 024305 (2011).

[23] M. Sugawara *et al.*, *Lifetime measurement for the possible antimagnetic rotation band in ^{101}Pd*, *Phys. Rev. C* **92**, 024309 (2015).

[24] N. Rather *et al.*, *Antimagnetic rotation in ^{104}Pd*, *Phys. Rev. C* **89**, 061303(R) (2014).

[25] C. Majumder *et al.*, *Possible Antimagnetic Rotational Band in ^{102}Ru*, *Braz. J. Phys.* **49**, 539 (2019).

[26] S. Ali *et al.*, *Evidence of antimagnetic rotation in an odd–odd nucleus: The case of ^{142}Eu*, *Phys. Rev. C* **96**, 021304(R) (2017).

[27] S. Rajbanshi *et al.*, *Antimagnetic rotation and sudden change of electric quadrupole transition strength in ^{143}Eu*, *Phys. Lett. B* **748**, 387 (2015).

[28] S. Chakraborty *et al.*, *Possible antimagnetic rotational band in ^{127}Xe*, *J. Phys. G.: Nucl. Part. Phys.* **47**, 015103 (2020).

[29] D.A. Torres *et al.*, *Deformations and magnetic rotations in the ^{60}Ni nucleus*, *Phys. Rev. C* **78**, 054318 (2008).

[30] P. Zhao *et al.*, *Novel structure for magnetic rotation bands in ^{60}Ni*, *Phys. Lett. B* **699**, 181 (2011).